(Fig. 2a). To examine whether the downstream signaling pathway was altered by the introduction of siRNA, the phosphorylation of ERK1/2 and AKT was examined. The phospho-ERK1/2 signal was significantly decreased by the suppression of CCDC6-RET expression, whereas the decrease of AKT phosphorylation was marginal (Fig. 2a). The involvement of RET fusion in LC-2/ad cell proliferation was then examined. The number of live CCDC6-RET-suppressed cells decreased throughout the experiment, and the difference became significant at day 3 and thereafter (Fig. 2b). To address the growth suppression further, the cell cycle of the siRNA-treated cells were assessed by the DNA ploidy pattern. The LC-2/ad cells treated with siRET exhibited significant increases in the percent of cells arrested in the G1 phase relative to the cells treated with siNC (Fig. 2c). However, the apoptotic cells, as assessed by Annexin V positivity, was not significantly increased by the suppression of RET expression (Fig. 2d).

RET-dependent transcriptome profile in LC-2/ad cell. To characterize the transcriptome profile, which is regulated by CCDC6-RET and its downstream signaling pathway, siRET#2 and siNC treated LC-2/ad cells were subjected to genome-wide expression profiling using Affymetrix U133Plus2.0 arrays. A total of 243 genes, evaluated with 285 probes were selected as those preferentially suppressed by less than half in siRET-treated cells.As well, 566 genes with 661 probes were expressed more than twice in siRET-treated cells (Table S2 and Fig. S3). The *RET* gene itself (probe ID = 211421_s_at) showed the highest fold-difference of 19.6 between siNC- and siRET#2-treated cells. Following *RET*, previously identified Gene Ontology-annotated Ras-MAPK downstream genes like *DUSP6* was preferentially suppressed in the siRET-treated cells. In addition, cell cycle regulation-related genes like *EREG, CDC6, MCM10, MAD2L1, CHEK1* and *PLK4* were expressed <0.5-fold in siRET-treated cells (Table 1).

RET fusion gene screening of 300 consecutive surgically resected LAD samples identified one case of *CCDC6-RET* expressing LAD by RT-PCR and break-apart FISH (Tsuta *et al.*, 2012, unpublished data). We checked the expression level of potential CCDC6-RET-driven genes identified above in the clinical sample. Among 285 preferentially expressed probes, 81 probes were also upregulated more than twofold in the *CCDC6-RET* positive LAD tissue compared to the surrounding non-cancerous tissue (Table 1 and Table S2).

RET inhibitor-induced cell cycle arrest and apoptosis in LC-2/ad cells. The phosphorylation status of the tyrosine 905 residue of RET isoforms 2 and 4 was high in the LC-2/ad cells, regardless of the presence or absence of serum in the culture medium, whereas the total amount of RET isoform 2 was not significantly altered. Similarly, the phosphorylation status of AKT and ERK1/2 was high under serum-starved conditions, and the enhanced phosphorylation of these molecules was slight with serum stimulation, suggesting that the fusion RET kinase was constitutively active and activated its downstream signaling pathways (Fig. 3a).

Next, the effects of kinase inhibitors, which inhibit spectrum including RET were applied to evaluate their effects on the signaling pathways in the LC-2/ad cells. We treated the cells with RET inhibitors vandetanib, sunitinib and sorafenib at a final concentration of 10 μM, which was 10–30 times higher than the *in vitro* half maximal inhibitory concentration (IC_{50}) for RET kinase activity of each compound. Gefitinib, another small molecule inhibitor targeting EGFR but not RET,[13] was also examined. All the inhibitors except gefitinib significantly suppressed the phosphorylation of RET, AKT and ERK1/2. Although vandetanib, sunitinib and sorafenib equivalently suppressed RET phosphorylation, vandetanib most significantly suppressed the phosphorylation of ERK1/2 (Fig. 3a). The inhibitory effect of vandetanib on RET, AKT and ERK1/2 phosphorylation exhibited concentration dependency (Fig. 3b). Gefitinib significantly suppressed EGFR phosphorylation while total EGFR protein level was not altered. Meanwhile, gefitinib did not alter the phosphorylation status of AKT and ERK1/2 (Fig. 3a). Meanwhile, vandetanib suppressed EGFR as well as AKT and ERK1/2 in *EGFR*-mutant PC-9 cells (Fig. S4).

We further examined the effect of the above inhibitors on the growth of the LC-2/ad cells using the WST-8 assay. Consistent with the effects of the inhibitors on the RET signaling pathway, vandetanib suppressed cell growth most significantly (IC_{50} = 0.32 μM), followed by sunitinib and sorafenib, whereas gefitinib only exhibited an apparent suppression at its highest dose (Fig. 3c). However, the effects of these inhibitors on *KRAS*-mutant A549 cells were much lower (Fig. S5). Gefitinib and vandetanib, both of which inhibit EGFR, suppressed *EGFR*-mutant PC-9 cells, whereas sunitinib and sorafenib had less effect (Fig. S5). Evaluating the number of live cells by trypan blue staining under the treatment of several doses of

Table 1. Up- or downregulated genes associated with mitogen-activated protein kinase (MAPK) cascade or cell cycle

Gene symbol	Probe set ID	siNC/siRET	Tumor/Non-tumor
Upregulated			
RET	211421_s_at	19.63	19.52
	205879_x_at	3.76	5.03
	215771_x_at	2.37	4.72
DUSP6	208892_s_at	4.45	5.22
	208893_s_at	4.17	6.34
	208891_at	4.17	3.56
EREG	1569583_at	3.68	1.60
	205767_at	2.93	5.69
CDC6	203967_at	2.42	4.82
	203968_s_at	1.95	5.32
MCM10	220651_s_at	2.30	4.83
	223570_at	1.72	1.71
MAD2L1	203362_s_at	2.28	5.91
	1554768_a_at	1.91	4.34
CHEK1	205394_at	2.17	9.03
	205393_s_at	2.14	6.87
PLK4	204886_at	2.07	4.38
	204887_s_at	1.56	4.08
Downregulated			
MEF2C	209200_at	0.21	0.46
	209199_s_at	0.26	0.65
GAB1	214987_at	0.23	0.42
	229114_at	0.53	0.65
	225998_at	0.62	0.68
	226002_at	0.64	0.76
CDKN1C	216894_x_at	0.26	0.41
	213348_at	0.32	0.23
	213183_s_at	0.35	0.30
	219534_x_at	0.42	0.27
	213182_x_at	0.44	0.21
PTEN	233314_at	0.33	0.27
	225363_at	0.77	0.47
TIMP2	231579_s_at	0.34	0.33
	224560_at	0.37	0.27
ID2	201566_x_at	0.35	0.31
	201565_s_at	0.40	0.39
	213931_at	0.52	0.31
CCNL2	232274_at	0.35	0.42
	222999_s_at	0.79	0.52
RPS6KA2	212912_at	0.41	0.34
	204906_at	0.59	0.49

vandetanib suggested a dose-dependent suppression in the LC-2/ad cells. Furthermore, the number of cells treated with 0.5 and 1.0 μM vandetanib was apparently reduced to less than the starting amount, strongly suggesting that vandetanib induced both cell death and the suppression of cell proliferation (Fig. 3d). An assessment of the DNA ploidy revealed that vandetanib arrested the cell cycle in G1 phase in a dose-dependent manner (Fig. 3e), and an increased concentration of vandetanib induced an Annexin V-positive apoptotic cell population (Fig. 3f). The proapoptotic effect of vandetanib was confirmed by the detection of cleaved caspase-3 by western blotting (Fig. 3b). Meanwhile, 1.0 μM sunitinib and sorafenib induced cell cycle arrest but induction of apoptosis was marginal (Figs S6 and S7).

To further evaluate the contribution of Ras-ERK and AKT axes to cell survival, LC-2/ad cells were treated with MEK1/2 inhibitor AZD6244 or PI3K/mTOR inhibitor BEZ235. Cytotoxic effect of AKT-inhibiting BEZ235 was more than that of ERK-inhibiting AZD6244. However, both inhibitors did not completely reduce the cell survival even their maximal dose (Figs S8 and S9).

Anti-tumor effect of vandetanib in an LC-2/ad xenograft model. Subcutaneously transplanted LC-2/ad tumors exhibited typical adenocarcinoma morphology. These tumors were positive for SFTPA, Napsin A and carcinoembryonic antigen (CEA) but thyroid marker thyroglobulin negative using immunohistochemistry (IHC). Furthermore, using an antibody cross-reacting with both human and mouse RET protein, IHC revealed that RET was highly expressed specifically in the tumor cells but not in the interstitial cells (Fig. 4a). The overexpression of RET in these tumors was confirmed using quantitative RT-PCR and Western blotting. Similar to the results from cultured LC-2/ad cells, much more mRNA of the 3′ end of *RET* was detected than that of the 5′ end (Fig. 4b), and a specific band equivalent to the size of the CCDC6-RET fusion protein was detected (Fig. 4c). Vandetanib (50 mg/kg) was orally administrated to the mice harboring the LC-2/ad xenograft, and the daily administration of vandetanib significantly reduced the tumor size. Although the tumors were diminished at day 14 of the treatment, the body weight of the treated mice was not significantly reduced (Fig. 4d and Fig. S10). Sorafenib (30 mg/kg) and sunitinib (40 mg/kg) did not reduce the body weight, either (Fig. S10). Sorafenib reduced but not diminished the tumors at day14. Anti-tumor effect of sunitinib was not significant (Fig. S11).

Discussion

Previous reports suggest that the incidence of *RET*-fusion-positive cases in LAD is 1–2% and that these cases are concentrated in the *EGFR* mutation-, *KRAS* mutation-, and *ALK*-fusion-negative population.[10,27] To identify cell lines expressing endogenous *RET*-fusion genes, we selected 11 cell lines that were derived from pathologically identified Japanese LAD cases. Among them, activating EGFR mutations have been reported in PC-3 and PC-9 cells.[28] However, the mutation status of known driver genes of other cell lines was not well investigated. The LC-2/ad cells were originally derived from pleural effusion of LAD in a patient who had received combined chemotherapy (endoxan, Adriamycin, Cisplatin and mitomycin C)[23]; the cancer was diagnosed by cytological examination of the patient's sputum and pleural effusion. The original report indicated that the LC-2/ad cells were positive for an adenocarcinoma marker, cytokeratin 18.[23] In addition, we detected surfactant protein, an aspartate proteinase, Napsin A, and CEA expression in the xenograft tumor (Fig. 4a). These findings support the origin of LC-2/ad as lung adenocarcinoma. The modal chromosome number described in the original report was 53–56, though an apparent translocation between the chromosomes was not reported, consistent with the fact that the inversion of chromosome 10 was not obvious in the conventional chromosome counts.

The Sanger sequencing in this study and the whole-transcriptome sequencing (Tsuchihara, 2012, unpublished data) revealed no driver mutations of *KRAS*, *EGFR* and known genes other than the *CCDC6-RET* fusion in the LC-2/ad cells, highly suggesting that the CCDC6-RET fusion protein plays pivotal roles in the proliferation of these cells. The autophosphorylation of CCDC6-RET was clearly observed in a serum-independent manner, accompanied with a constitutive elevation of ERK1/2 phosphorylation. The suppression of CCDC6-RET expression induced a decrease in ERK1/2 phosphorylation, accompanied with a decrease in the expression of the genes that regulate the cell cycle. As a result, the CCDC6-RET-suppressed cells exhibited significant growth retardation.

Recently, a Japanese group independently reported the CCDC6-RET fusion in LC2/ad cells.[21] However, the efficacy of RET inhibitors to the RET and downstream pathways and *in vivo* anti-tumor effects have been partially described.[21] Vandetanib, sorafenib and sunitinib suppress the activities of multiple kinases, including RET, and have been approved for several cancers.[29–31] In *in vitro* analyses, these compounds effectively suppressed the phosphorylation of CCDC6-RET and suppressed proliferation and induced death in LC-2/ad cells. It should be noted that the IC_{50} value for the growth suppression of these compounds was equivalent to the dose suggested in a previous study using culture cells expressing ectopic *KIF5B-RET* cDNA.[13] These effects were most likely dependent on RET inhibition. Sunitinib and sorafenib did not affect PC-9 and A549 cells, which have activating mutations of *EGFR* and *KRAS*, respectively. Vandetanib presumably suppressed the growth of PC-9 cells, as EGFR is included in its inhibitory spectrum. Meanwhile, gefitinib, which targets EGFR but not RET, did not significantly suppress the growth of LC-2/ad cells. Interestingly, gefitinib did not alter the phosphorylation of AKT and ERK1/2 in LC-2/ad cells albeit equivalently suppressing EGFR phosphorylation as vandetanib. Although precise molecular mechanisms should be further examined, LC-2/ad cells might not depend on EGFR for transducing downstream signaling.

Vandetanib exhibited apparent anti-tumor effects in the xenograft model in this study. Recently, efficacy of vandetanib on thyroid cancer cells harboring *RET*-fusion gene was also reported.[32] These findings strongly suggest that RET inhibition is a plausible therapeutic strategy for RET-fusion-positive tumors.

We noticed a discrepancy between the effects of RNA interference and inhibitor treatment on RET. Though RET suppression/inhibition equivalently reduced the level of phosphorylated RET and induced cell cycle arrest, obvious apoptosis was not found in the cells treated with siRNA. A possible explanation is that CCDC6-RET is mainly involved in the RAS-ERK pathway to regulate cell proliferation, whereas the anti-apoptotic signaling pathway mediated by AKT could be regulated by other signaling molecules inhibited by the multi-kinase inhibitors. A recent study using a Drosophila *in vivo* screening system suggested that the antitumor effects and toxicity of RET inhibitors were dependent on the profile of the "off-target" inhibition of multiple kinases in addition to the specific inhibition of RET.[33] Further investigation elucidating the molecules and signaling pathways relevant to the cytotoxic effect of vandetanib in LC-2/ad cells is anticipated.

Whether LC-2/ad-based models adequately represent clinical *RET* fusion-positive LAD cases is another challenging question. Takeuchi stated that clinically identified *CCDC6-RET*-positive LAD exhibited a histologically cribriform pattern.[14]

doi: 10.1111/cas.12175

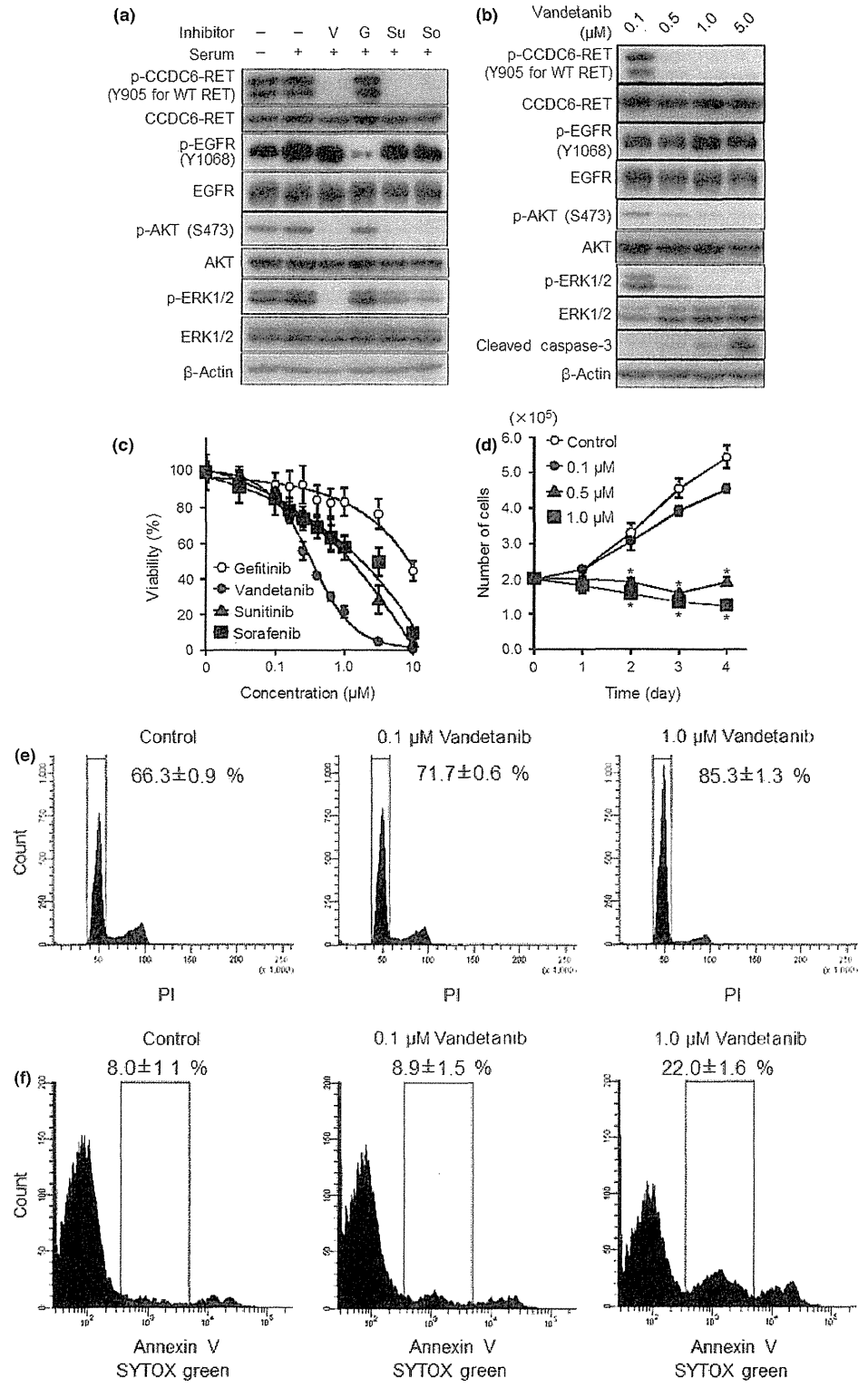

Fig. 3. Effect of RET inhibitors on LC-2/ad cells. (a) Western blot analysis of inhibitor-treated cells. The cells were incubated under serum-starved conditions for 22 h and treated with 1 μM of inhibitor or dimethylsulfoxide (DMSO) for 2 h. Prior to cell lysis, the cells were treated with 10% fetal bovine serum (FBS) for 10 min. Whole-cell lysates were subjected to western blot analysis to detect the indicated proteins. G, gefitinib; So, sorafenib; Su, sunitinib; V, vandetanib. (b) Dose-dependent effect of vandetanib. Cells were treated with the indicated concentration of vandetanib for 12 h, and western blotting was used to detect the indicated proteins. (c) WST-8 assay with kinase inhibitors. Cells were treated with the indicated inhibitors for 72 h, and the viability was assessed using the WST-8 assay. The data are shown as the mean ± standard deviation (SD) ($n = 6$). (d) Effect of vandetanib for growth inhibition. Cells were treated with vandetanib and incubated for the indicated time. The data are shown as the mean ± SD ($n = 3$). *$P < 0.01$ (Student's t test). (e,f) DNA ploidy (e) and Annexin V-positive population (f) of the cells treated with vandetanib for 48 h. The data are shown as the mean ± SD ($n = 4$).

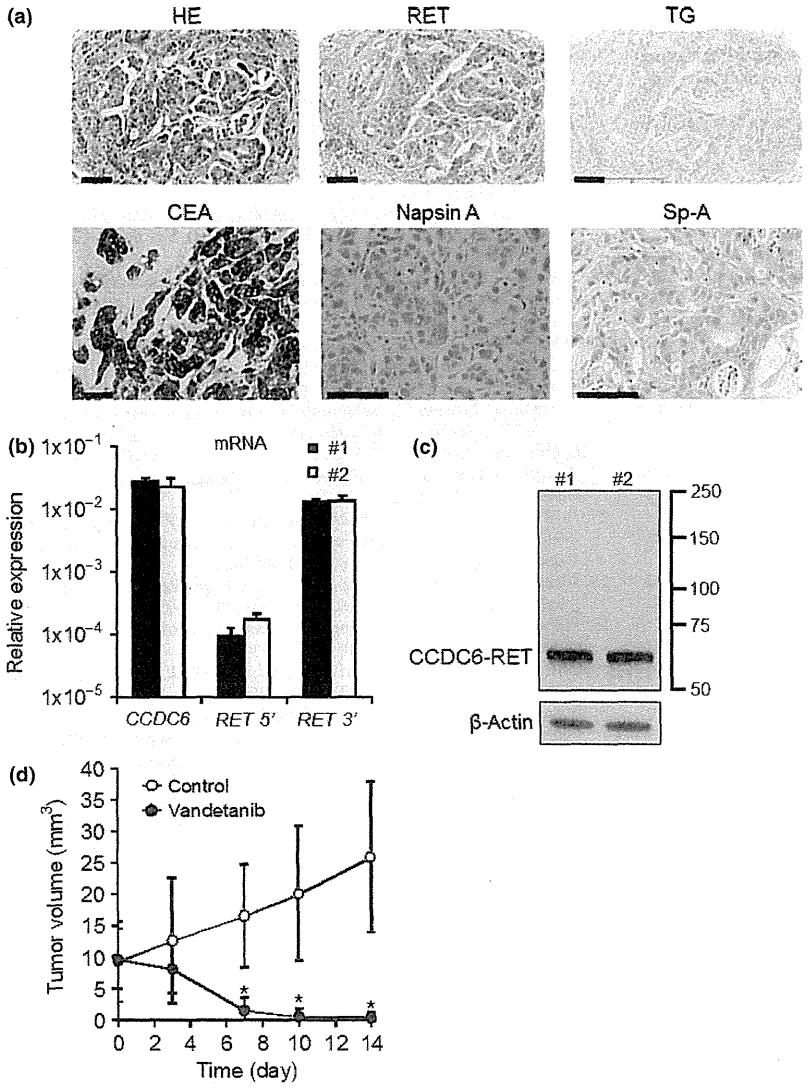

Fig. 4. Characterization of the LC-2/ad xenograft and anti-tumor effects of vandetanib. (a) Histological features of the xenograft. Hematoxylin and eosin staining and immunohistochemical staining with the indicated antibodies. Scale bars were 100 μm. Hematoxylin eosin (HE), RET, thyroglobulin (TG) and carcinoembryonic antigen (CEA) (×20); Napsin A and Sp-A (×40). (b) 3′ region-specific expression of *RET* mRNA in the xenograft. Total RNA extracted from tumors was subjected to real-time reverse transcription-polymerase chain reaction (RT-PCR) analysis with the primer sets designed for the 5′ or 3′ region of the *RET* and *CCDC6* cDNA. The data are shown as the mean ± standard deviation (SD) ($n = 3$). (c) Expression of the CCDC6-RET protein in mice xenografts. Whole-cell lysates of tumors were subjected to western blot analysis. (d) Anti-tumor effect of vandetanib *in vivo*. Vandetanib was administered once a day at a dosage of 50 mg/kg. The data are shown as the mean ± SD ($n = 9$). *$P < 0.01$ (control *vs* sorafenib; Student's *t* test).

Because the cribriform structure was presumably developed from normal alveolar architecture, this specific morphology was not observed in the subcutaneously transplanted LC-2/ad tumors. We assume that the comparison of the transcriptome profile between the LC-2/ad cells and clinically identified LAD tissue samples may provide clues. Approximately one-third of the genes suppressed by RNA interference directed at *RET* overlapped with the genes preferentially expressed in the clinical tumor sample. Because we have had only one example of paired data, it is difficult to estimate the similarity between the cell line and clinical samples. However, the above overlap appears promising, and we will continue to screen both cell lines and clinical samples to accumulate comprehensive data.

In this study, the screening of Japanese LAD cell lines was effective for the identification of *RET* fusion-positive cancer cells, representing a clinically rare subpopulation. LC-2/ad cells might be useful in the development of RET-targeted therapies, that is, new compound screening, clarifying the pharmacological mechanisms and investigating the mechanisms for acquired resistance.

Acknowledgments

We thank Drs Hiroki Sasaki and Kazuhiko Aoyagi and the National Cancer Center Research Core Facility for the microarray analyses. The Core Facility was supported by National Cancer Center Research and Development Fund (23-A-7). This work was supported by National Cancer Center Research and Development Fund (23-A-8, 15, 24-A-1) and JSPS KAKENHI Grant number 24300345.

Disclosure Statement

The authors have no conflict of interest.

References

1 Jemal A, Bray F, Center MM, Ferlay J, Ward E, Forman D. Global cancer statistics. *CA Cancer J Clin* 2011; **61**: 69–90.

2 Pao W, Girard N. New driver mutations in non-small-cell lung cancer. *Lancet Oncol* 2011; **12**: 175–80.

3 Pao W, Chmielecki J. Rational, biologically based treatment of EGFR-mutant non-small-cell lung cancer. *Nat Rev Cancer* 2010; **10**: 760–74.

doi: 10.1111/cas.12175

4 Kwak EL, Bang YJ, Camidge DR *et al.* Anaplastic lymphoma kinase inhibition in non-small-cell lung cancer. *N Engl J Med* 2010; **363**: 1693–703.
5 Lynch TJ, Bell DW, Sordella R *et al.* Activating mutations in the epidermal growth factor receptor underlying responsiveness of non-small-cell lung cancer to gefitinib. *N Engl J Med* 2004; **350**: 2129–39.
6 Paez JG, Janne PA, Lee JC *et al.* EGFR mutations in lung cancer: correlation with clinical response to gefitinib therapy. *Science* 2004; **304**: 1497–500.
7 Tsao MS, Sakurada A, Cutz JC *et al.* Erlotinib in lung cancer – molecular and clinical predictors of outcome. *N Engl J Med* 2005; **353**: 133–44.
8 Govindan R, Ding L, Griffith M *et al.* Genomic landscape of non-small cell lung cancer in smokers and never-smokers. *Cell* 2012; **150**: 1121–34.
9 Imielinski M, Berger AH, Hammerman PS *et al.* Mapping the hallmarks of lung adenocarcinoma with massively parallel sequencing. *Cell* 2012; **150**: 1107–20.
10 Seo JS, Ju YS, Lee WC *et al.* The transcriptional landscape and mutational profile of lung adenocarcinoma. *Genome Res* 2012; **22**: 2109–19.
11 Kohno T, Ichikawa H, Totoki Y *et al.* KIF5B-RET fusions in lung adenocarcinoma. *Nat Med* 2012; **18**: 375–7.
12 Li F, Feng Y, Fang R *et al.* Identification of *RET* gene fusion by exon array analyses in "pan-negative" lung cancer from never smokers. *Cell Res* 2012; **22**: 928–31.
13 Lipson D, Capelletti M, Yelensky R *et al.* Identification of new *ALK* and *RET* gene fusions from colorectal and lung cancer biopsies. *Nat Med* 2012; **18**: 382–4.
14 Takeuchi K, Soda M, Togashi Y *et al.* RET, ROS1 and ALK fusions in lung cancer. *Nat Med* 2012; **18**: 378–81.
15 Wang R, Hu H, Pan Y *et al.* RET fusions define a unique molecular and clinicopathologic subtype of non-small-cell lung cancer. *J Clin Oncol* 2012; **30**: 4352–9.
16 Gardner E, Papi L, Easton DF *et al.* Genetic linkage studies map the multiple endocrine neoplasia type 2 loci to a small interval on chromosome 10q11.2. *Hum Mol Genet* 1993; **2**: 241–6.
17 Mole SE, Mulligan LM, Healey CS, Ponder BA, Tunnacliffe A. Localisation of the gene for multiple endocrine neoplasia type 2A to a 480 kb region in chromosome band 10q11.2. *Hum Mol Genet* 1993; **2**: 247–52.
18 Mulligan LM, Kwok JB, Healey CS *et al.* Germ-line mutations of the RET proto-oncogene in multiple endocrine neoplasia type 2A. *Nature* 1993; **363**: 458–60.
19 Hofstra RM, Landsvater RM, Ceccherini I *et al.* A mutation in the RET proto-oncogene associated with multiple endocrine neoplasia type 2B and sporadic medullary thyroid carcinoma. *Nature* 1994; **367**: 375–6.
20 Grieco M, Cerrato A, Santoro M, Fusco A, Melillo RM, Vecchio G. Cloning and characterization of H4 (D10S170), a gene involved in RET rearrangements *in vivo*. *Oncogene* 1994; **9**: 2531–5.
21 Matsubara D, Kanai Y, Ishikawa S *et al.* Identification of CCDC6-RET fusion in the human lung adenocarcinoma cell line, LC-2/ad. *J Thorac Oncol* 2012; **7**: 1872–6.
22 Makinoshima H, Ishii G, Kojima M *et al.* PTPRZ1 regulates calmodulin phosphorylation and tumor progression in small-cell lung carcinoma. *BMC Cancer* 2012; **12**: 537.
23 Kataoka H, Itoh H, Seguchi K, Koono M. Establishment and characterization of a human lung adenocarcinoma cell line (LC-2/ad) producing alpha 1-antitrypsin *in vitro*. *Acta Pathol Jpn* 1993; **43**: 566–73.
24 Wedge SR, Ogilvie DJ, Dukes M *et al.* ZD6474 inhibits vascular endothelial growth factor signaling, angiogenesis, and tumor growth following oral administration. *Cancer Res* 2002; **62**: 4645–55.
25 Yoshida A, Tsuta K, Nakamura H *et al.* Comprehensive histologic analysis of ALK-rearranged lung carcinomas. *Am J Surg Pathol* 2011; **35**: 1226–34.
26 Okayama H, Kohno T, Ishii Y *et al.* Identification of genes upregulated in ALK-positive and EGFR/KRAS/ALK-negative lung adenocarcinomas. *Cancer Res* 2012; **72**: 100–11.
27 Ju YS, Lee WC, Shin JY *et al.* A transforming *KIF5B* and *RET* gene fusion in lung adenocarcinoma revealed from whole-genome and transcriptome sequencing. *Genome Res* 2012; **22**: 436–45.
28 Blanco R, Iwakawa R, Tang M *et al.* A gene-alteration profile of human lung cancer cell lines. *Hum Mutat* 2009; **30**: 1199–206.
29 Phay JE, Shah MH. Targeting RET receptor tyrosine kinase activation in cancer. *Clin Cancer Res* 2010; **16**: 5936–41.
30 Antonelli A, Fallahi P, Ferrari SM *et al.* RET TKI: potential role in thyroid cancers. *Curr Oncol Rep* 2012; **14**: 97–104.
31 Scagliotti GV. Potential role of multi-targeted tyrosine kinase inhibitors in non-small-cell lung cancer. *Ann Oncol* 2007; **18**(Suppl 10): x32–41.
32 Couto JP, Almeida A, Daly L *et al.* AZD1480 blocks growth and tumorigenesis of RET- activated thyroid cancer cell lines. *PLoS ONE* 2012; **7**: e46869.
33 Dar AC, Das TK, Shokat KM, Cagan RL. Chemical genetic discovery of targets and anti-targets for cancer polypharmacology. *Nature* 2012; **486**: 80–4.

Supporting Information

Additional Supporting Information may be found in the online version of this article:

Data S1. Materials and methods.

Fig. S1. The absence of the known driver mutations.

Fig. S2. Suppression of *RET* mRNA in siRET-treated cells.

Fig. S3. RET-dependent transcriptome profile in LC-2/ad cells.

Fig. S4. Dose-dependent effect of vandetanib in PC-9 cells.

Fig. S5. WST-8 assay with various kinase inhibitors.

Fig. S6. Effect of sunitinib and sorafenib on G1 phase population of LC-2/ad cells.

Fig. S7. Effect of sunitinib and sorafenib on apoptosis of LC-2/ad cells.

Fig. S8. Dose-dependent effect of AZD6244 and BEZ235 in LC-2/ad cells.

Fig. S9. WST-8 assay of LC-2/ad cells treated with AZD6244 and BEZ235.

Fig. S10. Body weight of the vandetanib-, sunitinib-, sorafenib- and vehicle-treated mice.

Fig. S11. Effect of sunitinib and sorafenib *in vivo*.

Table S1. Polymerase chain reaction primers.

Table S2. Summary of the microarray data.